Chapter 2

PAPR Reduction in WiMAX System

Mona Shokair and Hifzalla Sakran

Additional information is available at the end of the chapter

http://dx.doi.org/10.5772/55380

1. Introduction

Broadband Wireless Access (BWA) has emerged as a promising solution for last mile access technology to provide high speed internet access in the residential as well as small and medium sized enterprise sectors. At this moment, cable and DSL technologies are providing broadband service in these sectors. But the practical difficulties in deployment have prevented them from reaching many potential broadband internet customers. Many areas throughout the world currently are not under broadband access facilities. Even many urban and suburban locations may not be served by DSL connectivity as it can only reach about three miles from the central office switch [1]. On the other side many older cable networks do not have return channel which will prevent to offer internet access and many commercial areas are often not covered by cable network. But with BWA this difficulties can be overcomed. Because of its wireless nature, it can be faster to deploy, easier to scale and more flexible, thereby giving it the potential to serve customers not served or not satisfied by their wired broadband alternatives.

IEEE 802.16 standard for BWA and its associated industry consortium, Worldwide Interoperability for Microwave Access (WiMAX) forum promise to offer high data rate over large areas to a large number of users where broadband is unavailable. This is the first industry wide standard that can be used for fixed wireless access with substantially higher bandwidth than most cellular networks [2]. Wireless broadband systems have been in use for many years, but the development of this standard enables economy of scale that can bring down the cost of equipment, ensure interoperability, and reduce investment risk for operators.

The first version of the IEEE 802.16 standard operates in the 10–66GHz frequency band and requires line of sight (LOS) towers. Later the standard extended its operation through different PHY specification to 2-11 GHz frequency band enabling non line of sight (NLOS) connections, which require techniques that efficiently mitigate the impairment of fading and multipath [3]. Taking the advantage of OFDM technique the PHY is able to provide robust broadband service

in hostile wireless channel. The OFDM based physical layer of the IEEE 802.16 standard has been standardized in close cooperation with the European Telecommunications Standards Institute (ETSI) High PERformance Metropolitan Area Network (HiperMAN) [4]. Thus, the HiperMAN standard and the OFDM based physical layer of IEEE 802.16 are nearly identical. Both OFDM based physical layers shall comply with each other and a global OFDM system should emerge [5]. The WiMAX forum certified products for BWA comply with the both standards.

Some researchers investigate the effect of nonlinear amplifier in WiMAX [6] and apply Clipping as a simple method [7], CORDIC Algorithm [8], and Tone Reservation [9] to reduce PAPR in WiMAX system.

In this chapter, proposed WiMAX system will be studied. This system will be compared with the conventional system. Where the companding technique is used to reduce PAPR based on the properties of the μ-law that uses for decreasing dynamics range of the signal. Moreover, the performance of the proposed system will be compared with the system that uses clipping as a reduction of PAPR. These systems will be investigated under SUI channels and AWGN.

In Section 1.2, the broadband channel will be explained. In section 1.3 SUI multipath Channel Models will be investigated. The performance of MMSE equalizer over SUI model will be study in section 1.4. In section 1.5, a system model of WiMAX for PAPR will be explained. PAPR Reduction Technique Using μ-Law Compander is studied in Section 1.6. Finally, summary will be made.

2. Broadband wireless channel models

One of the more intriguing aspects of wireless channels is fading. Unlike path loss or shadowing, which are large-scale attenuation effects owing to distance or obstacles, fading is caused by the reception of multiple versions of the same signal. The multiple received versions are caused by reflections that are referred to as *multipath*. The reflections may arrive nearly simultaneously— for example, if there is local scattering around the receiver—or at relatively longer intervals— for example, owing to multiple paths between the transmitter and the receiver (Figure 1).

When some of the reflections arrive at nearly the same time, their combined effect is as in Figure 2. Depending on the phase difference between the arriving signals, the interference can be either constructive or destructive, which causes a very large observed difference in the amplitude of the received signal even over very short distances. In other words, moving the transmitter or the receiver even a very short distance can have a dramatic effect on the received amplitude, even though the path loss and shadowing effects may not have changed at all.

One of the key parameters in the design of a transmission system is the maximum delay spread value that it has to tolerate.

In order to design and benchmark wireless communication systems, it is important to develop channel models that incorporate their variations in time, frequency, and space. Models are

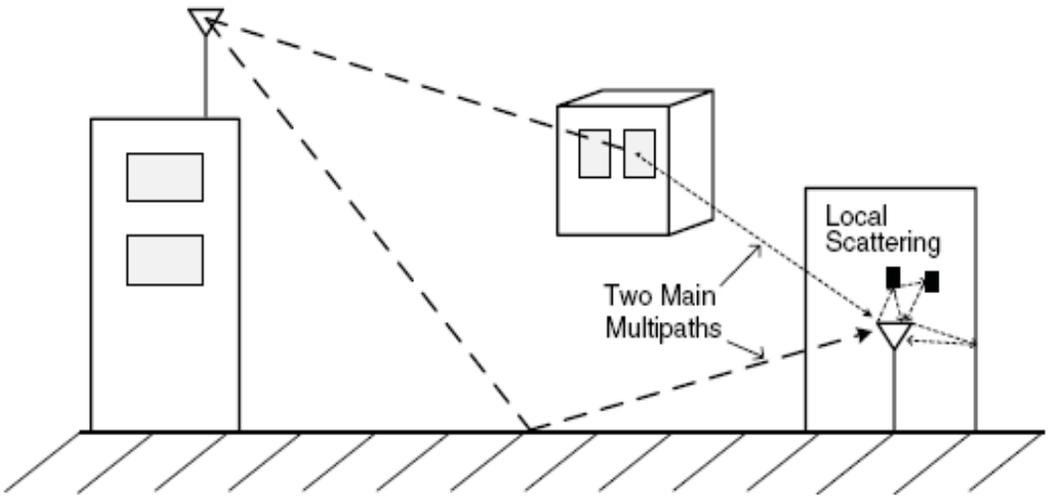

Figure 1. A channel with a few major paths of different lengths, with the receiver seeing a number of locally scattered versions of those paths.

classified as either *statistical* or *empirical*. Statistical models are simpler and are useful for analysis and simulations. Empirical models are more complicated but usually represent a specific type of channel more accurately. There are several channels models which are explained in the following,

2.1. Statistical channel models

As we have noted, the received signal in a wireless system is the superposition of numerous reflections, or multipath components. The reflections may arrive very closely spaced in time — for example, if there is local scattering around the receiver—or at relatively longer intervals.

Figure 2 shows that when the reflections arrive at nearly the same time, constructive and destructive interference between the reflections causes the envelope of the aggregate received signal r(t) to vary substantially.

In this section, we summarize statistical methods for characterizing the amplitude and power of r(t) when all the reflections arrive approximately at the same time.

2.1.1. Rayleigh fading

Suppose that the number of scatters is large and that the angles of arrival between them are uncorrelated. From the Central Limit Theorem, it can be shown that the in-phase (cosine) and quadrature (sine) components of r(t), denoted as $r_I(t)$ and $r_Q(t)$, follow two independent time correlated Gaussian random processes.

Consider a snapshot value of at time t =0, and note that $r(0)= r_I(0) + r_Q(0)$. Since the values $r_I(0)$ and $r_Q(0)$ are Gaussian random variables, it can be shown that the distribution of the envelope

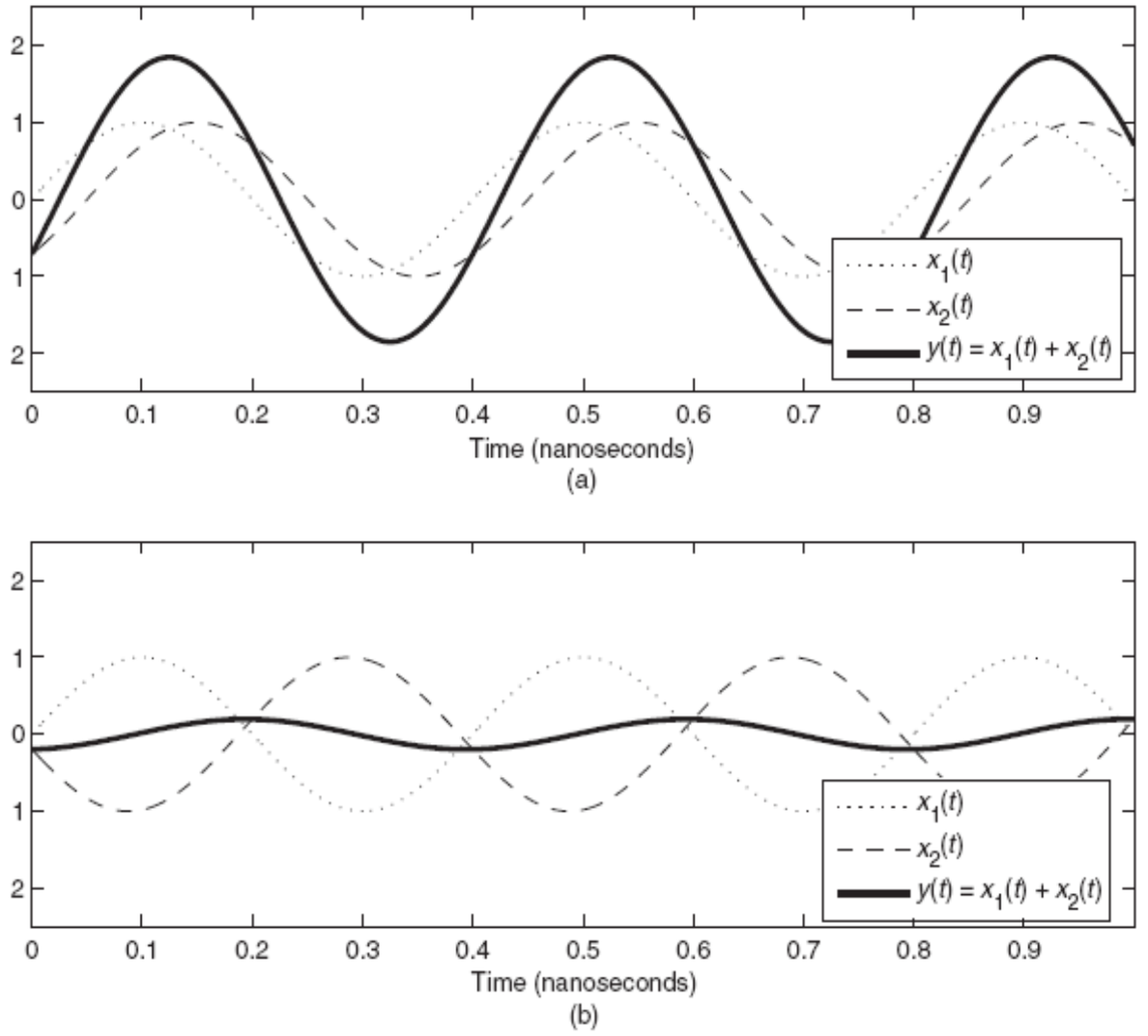

Figure 2. The difference between (a) constructive interference and (b) destructive interference at *fc* = 2.5GHz is less than 0.1 nanoseconds in phase, which corresponds to about 3 cm.

amplitude $|r| = \sqrt{r_I^2 + r_Q^2}$ is Rayleigh and that the received power $|r|^2 = r_I^2 + r_Q^2$ is exponentially distributed. Formally [10],

$$f_{|r|}(x) = \frac{2x}{p_r} e^{-x^2/p_r} \quad , \quad x \geq 0, \tag{1}$$

and

$$f_{|r|^2}(x) = \frac{2x}{p_r} e^{-x/p_r} \quad , \quad x \geq 0, \tag{2}$$

where p_r is the average received power.

2.1.2. LOS channels: Ricean distribution

An important assumption in the Rayleigh fading model is that all the arriving reflections have a mean of zero. This will not be the case if there is a dominant path—for example, a LOS path — between the transmitter and the receiver. For a LOS signal, the received envelope distribution is more accurately modeled by a Ricean distribution, which is given by

$$f_{|r|}(x) = \frac{x}{\sigma^2} e^{-(x^2+\mu^2)/2\sigma^2} I_0\left(\frac{x\mu}{\sigma^2}\right) \quad , \quad x \geq 0, \tag{3}$$

where μ^2 is the power of the LOS component, σ^2 is the variance and I_0 is the 0^{th}-order, modified Bessel function of the first kind. Although more complicated than a Rayleigh distribution, this expression is a generalization of the Rayleigh distribution. This can be confirmed by observing that

$$\mu = 0 \Rightarrow I_0\left(\frac{x\mu}{\sigma^2}\right) = 1 \quad ,$$

Therefore the Ricean distribution reduces to the Rayleigh distribution in the absence of a LOS component.

Since the Ricean distribution depends on the LOS component's power μ^2, a common way to characterize the channel is by the relative strengths of the LOS and scattered paths. This factor, *K*, is quantified as

$$K = \frac{\mu^2}{2\sigma^2}$$

and is a natural description of how strong the LOS component is relative to the NLOS components.
For $K = 0$, the Ricean distribution again reduces to Rayleigh, and as $K \to \infty$, the physical meaning is that there is only a single LOS path and no other scattering. Mathematically, as K grows large, the Ricean distribution is quite Gaussian about its mean μ with decreasing variance, physically meaning that the received power becomes increasingly deterministic.

The average received power under Ricean fading is the combination of the scattering power and the LOS power: $P_r = 2\sigma^2 + \mu^2$. Although it is not straightforward to directly find the Ricean power distribution $f_{|r|^2}(x)$, the Ricean envelope distribution in terms of K can be found by substituting $\mu^2 = K P_r / (K+1)$ and $2\sigma^2 = P_r / (K+1)$ into Equation (3).

Although its simplicity makes the Rayleigh distribution more amenable to analysis than the Ricean distribution, the Ricean distribution is usually a more accurate depiction of wireless broadband systems, which typically have one or more dominant components. This is espe-

cially true of fixed wireless systems, which do not experience fast fading and often are deployed to maximize LOS propagation.

2.2. Empirical channel models

The parametric statistical channel models discussed therefore in this chapter do not take into account specific wireless propagation environments. Although exactly modeling a wireless channel requires complete knowledge of the surrounding scatterers, such as buildings and plants, the time and computational demands of such a methodology are unrealistic, owing to the near-infinite number of possible transmit/receive locations and the fact that objects are subject to movement. Therefore, empirical and semiempirical wireless channel models have been developed to accurately estimate the path loss, shadowing, and small-scale fast fading. Although these models are generally not analytically tractable, they are very useful for simulations and to fairly compare competing designs. Empirical models are based on extensive measurement of various propagation environments, and they specify the parameters and methods for modeling the typical propagation scenarios in various wireless systems.

2.3. Stanford University Interim (SUI) channel models

SUI channel models are an extension of the earlier work by AT&T Wireless and Erceg. In this model a set of six channels was selected to address three different terrain types that are typical of the continental US [11]. This model can be used for simulations, design, development and testing of technologies suitable for fixed broadband wireless applications [12]. The parameters for the model were selected based upon some statistical models. The tables below depict the parametric view of the six SUI channels.

TerrainType	SUIChannels
C (Mostly flat terrain with light tree densities)	SUI1, SUI2
B (Hilly terrain with light tree density or flat terrain with moderate to heavy tree density)	SUI3, SUI4
A (Hilly terrain with moderate to heavy tree density)	SUI5, SUI6

Table 1. Terrain type for SUI channel.

The parametric view of the SUI channels is summarized in the Table 2. For simplicity, SUI 1 from train type C(Flat/Light tree density), SUI 3 from train type B(Hilly/Light tree density or Flat/moderate tree density),and SUI 5 from train type A(Hilly/moderate to heavy tree density) are considered in the following.

Model	Delay	L(numberoftape)=3			RMS Delay spread
Gain		Tap1	Tap2	Tap3	
Kfactor					
SUI 1		0 μs	0.4 μs	0.9 μs	0.111 μs
		0 dB	-15 dB	-20 dB	
		4	0	0	
SUI 2		0 μs	0.4 μs	1.1 μs	0.202 μs
		0 dB	-12 dB	-15 dB	
		2	0	0	
SUI 3		0 μs	0.4 μs	0.9 μs	0.264 μs
		0 dB	-5 dB	-10 dB	
		1	0	0	
SUI 4		0 μs	1.5 μs	4 μs	1.257 μs
		0 dB	-4 dB	-8 dB	
		0	0	0	
SUI 5		0 μs	4 μs	10 μs	2.842 μs
		0 dB	-5 dB	-10 dB	
		0	0	0	
SUI 6		0 μs	14 μs	20 μs	5.240 μs
		0 dB	-10 dB	-14 dB	
		0	0	0	

Table 2. SUI Channels Parameter.

3. Equalization in wireless channel

Equalization defines any signal processing technique used at the receiver to alleviate the ISI problem caused by delay spread. Signal processing can also be used at the transmitter to make the signal less susceptible to delay spread: spread spectrum and multicarrier modulation fall in this category of transmitter signal processing techniques. ISI mitigation is required when the modulation symbol time T_s is on the order of the channel's rms delay spread σ_{Tm}. Higher data rate applications are more sensitive to delay spread, and generally require high-performance equalizers or other ISI mitigation techniques. In fact, mitigating the applications are more sensitive to delay spread, and generally require high-performance equalizers or other ISI mitigation techniques. In fact, mitigating the applications are more sensitive to delay spread, and generally require high-performance equalizers or other ISI mitigation techniques. In fact, mitigating the impact of delay spread is one of the most challenging hurdles for high-speed wireless data systems.

Equalizer design must typically balance ISI mitigation with noise enhancement, since both the signal and the noise pass through the equalizer, which can increase the noise power. Nonlinear

equalizers suffer less from noise enhancement than linear equalizers, but typically entail higher complexity.

Equalization techniques fall into two broad categories: linear and nonlinear. The linear techniques are generally the simplest to implement and to understand conceptually. However, linear equalization techniques typically suffer from more noise enhancement than nonlinear equalizers.

Among nonlinear equalization techniques, decision-feedback equalization (DFE) is the most common, since it is fairly simple to implement and generally performs well. However, on channels with low SNR, the DFE suffers from error propagation when bits are decoded in error, leading to poor performance. The optimal equalization technique is maximum likelihood sequence estimation (MLSE). Unfortunately, the complexity of this technique grows exponentially with the length of the delay spread, and is therefore impractical on most channels of interest.

However, the performance of the MLSE is often used as an upper bound on performance for other equalization techniques.

It is clear that equalization in OFDM can be very simple. This is one of the major advantages of using OFDM over single carrier systems. Channel equalization in OFDM actually can be done by just a simple division in the frequency domain. This is because the channel as a filter is convolved with the input signal in the time domain on transmission. This operation is equivalent to multiplication in the frequency domain and thus undoing the effects of the channel is just a division.

This section studies the performance of OFDM system over multipath SUI channels which are not clarified until now. Moreover, the performance of this system will be compared with the performance of the system with the frequency domain equalizer (FDE) using MMSE. Also this system will be investigated over AWGN.

3.1. System model

The OFDM implementation of multicarrier modulation is shown in Figure 3. The input data stream is modulated by a QAM modulator, resulting in a complex symbol stream $X[0],X[1],...,X[N-1]$ of length N. This symbol stream is passed through a serial-to-parallel converter, whose output is a set of N parallel QAM symbols $X[0],..., X[N-1]$ corresponding to the symbols transmitted over each of the subcarriers. Thus, the N symbols output from the serial-to-parallel converter are the discrete frequency components of the OFDM modulator output $s(t)$. In order to generate $s(t)$, these frequency components are converted into time samples by performing an inverse DFT on these N symbols, which is efficiently implemented using the IFFT algorithm. The IFFT yields the OFDM symbol consisting of the sequence $x[n] = X[0],..., x[N-1]$ of length N, where

$$x(n) = \sum_{i=0}^{N-1} X(i) e^{j2\pi ni/N}, 0 \le n \le N-1. \quad (4)$$

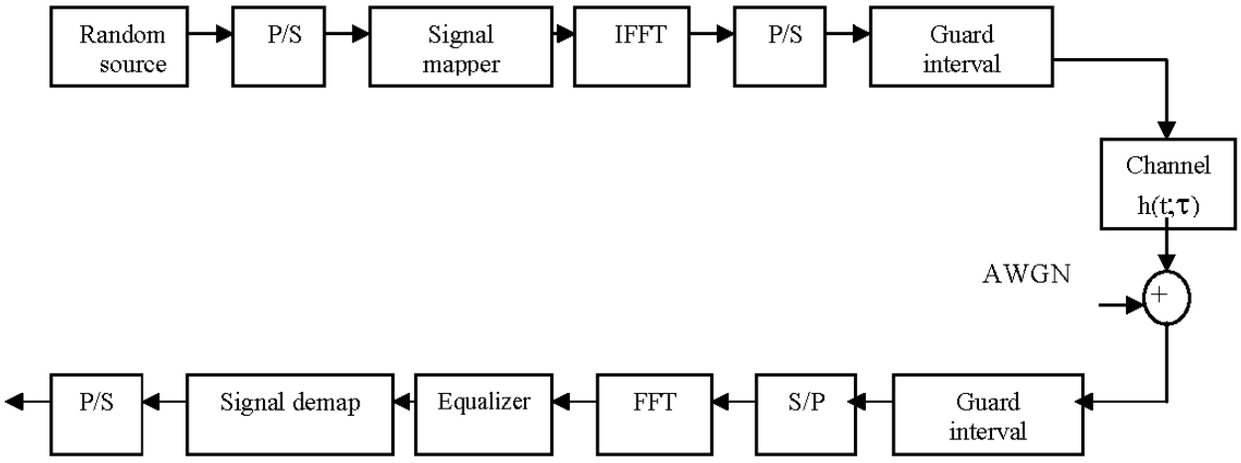

Figure 3. Model for studied OFDM-system.

This sequence corresponds to samples of the multicarrier signal: i.e. the multicarrier signal consists of linearly modulated subchannels, and the right hand side of (4) corresponds to samples of a sum of QAM symbols $X[i]$ each modulated by carrier frequency. The cyclic prefix is then added to the OFDM symbol, and the resulting time samples $\tilde{x}[n] = \tilde{x}[-\mu],\ldots, \tilde{x}[N-1] = x[N-\mu],\ldots, x[0],\ldots, x[N-1]$ are ordered by the parallel-to-serial converter[13].

The received signal is $r[n] = \tilde{x}[n] * h[n] + v[n], -\mu \le n \le N-1$.

Where $h(n)$ is impulse response of channel with length $\mu + 1 = T_m/T_s$, where T_m is the channel delay spread and T_s the sampling time associated with the discrete time sequence, $v[n]$ is AWGN.

To simplify our derivation, we will choose N =8 subcarriers, prefix-length=2. Assume channel impulse response is : $h_0,h_1,h_2,0,0\ldots$.

Received samples for symbol m, after removing prefix:

$$\underbrace{\begin{bmatrix} r_m^0 \\ r_m^1 \\ r_m^2 \\ r_m^3 \\ r_m^4 \\ r_m^5 \\ r_m^6 \\ r_m^7 \end{bmatrix}}_{\text{received samples for symbol m}} = \underbrace{\begin{bmatrix} h_2 & h_1 & h_0 & 0 & 0 & 0 & 0 & 0 & 0 & 0 \\ 0 & h_2 & h_1 & h_0 & 0 & 0 & 0 & 0 & 0 & 0 \\ 0 & 0 & h_2 & h_1 & h_0 & 0 & 0 & 0 & 0 & 0 \\ 0 & 0 & 0 & h_2 & h_1 & h_0 & 0 & 0 & 0 & 0 \\ 0 & 0 & 0 & 0 & h_2 & h_1 & h_0 & 0 & 0 & 0 \\ 0 & 0 & 0 & 0 & 0 & h_2 & h_1 & h_0 & 0 & 0 \\ 0 & 0 & 0 & 0 & 0 & 0 & h_2 & h_1 & h_0 & 0 \\ 0 & 0 & 0 & 0 & 0 & 0 & 0 & h_2 & h_1 & h_0 \end{bmatrix}}_{\text{channel matrix}} \underbrace{\begin{bmatrix} x_m^6 \\ x_m^7 \\ x_m^0 \\ x_m^1 \\ x_m^2 \\ x_m^3 \\ x_m^4 \\ x_m^5 \\ x_m^6 \\ x_m^7 \end{bmatrix}}_{\text{transmitted sequence for symbol m}} \quad (5)$$

This is equivalent with:

$$\underbrace{\begin{bmatrix} r_m^0 \\ r_m^1 \\ r_m^2 \\ r_m^3 \\ r_m^4 \\ r_m^5 \\ r_m^6 \\ r_m^7 \end{bmatrix}}_{\text{received samples for symbol m}} = \underbrace{\begin{bmatrix} h_0 & 0 & 0 & 0 & 0 & 0 & h_2 & h_1 \\ h_1 & h_0 & 0 & 0 & 0 & 0 & 0 & h_2 \\ h_2 & h_1 & h_0 & 0 & 0 & 0 & 0 & 0 \\ 0 & h_2 & h_1 & h_0 & 0 & 0 & 0 & 0 \\ 0 & 0 & h_2 & h_1 & h_0 & 0 & 0 & 0 \\ 0 & 0 & 0 & h_2 & h_1 & h_0 & 0 & 0 \\ 0 & 0 & 0 & 0 & h_2 & h_1 & h_0 & 0 \\ 0 & 0 & 0 & 0 & 0 & h_2 & h_1 & h_0 \end{bmatrix}}_{\text{modified channel matrix}} \cdot \begin{bmatrix} x_m^0 \\ x_m^1 \\ x_m^2 \\ x_m^3 \\ x_m^4 \\ x_m^5 \\ x_m^6 \\ x_m^7 \end{bmatrix} \tag{6}$$

The modified channel matrix is a so-called "circulant" matrix (constant along the diagonals & wrapped around). For every circulant matrix C is diagonalized by a DFT & I-DFT matrix:

$C = (IDFT).(\text{diagonal matrix}).(DFT)$

Diagonal matrix has DFT of first column of C on its main diagonal

By substituting this:

$$\underbrace{DFT.\begin{bmatrix} r_m^0 \\ r_m^1 \\ r_m^2 \\ r_m^3 \\ r_m^4 \\ r_m^5 \\ r_m^6 \\ r_m^7 \end{bmatrix}}_{\text{received symbol in freq.domain}} = \underbrace{\begin{bmatrix} H_0 & 0 & 0 & 0 & 0 & 0 & 0 & 0 \\ 0 & H_1 & 0 & 0 & 0 & 0 & 0 & 0 \\ 0 & 0 & H_2 & 0 & 0 & 0 & 0 & 0 \\ 0 & 0 & 0 & H_3 & 0 & 0 & 0 & 0 \\ 0 & 0 & 0 & 0 & H_4 & 0 & 0 & 0 \\ 0 & 0 & 0 & 0 & 0 & H_5 & 0 & 0 \\ 0 & 0 & 0 & 0 & 0 & 0 & H_6 & 0 \\ 0 & 0 & 0 & 0 & 0 & 0 & 0 & H_7 \end{bmatrix}}_{\text{channel matrix in freq.domain}} \cdot \begin{bmatrix} X_m^0 \\ X_m^1 \\ X_m^2 \\ X_m^3 \\ X_m^4 \\ X_m^5 \\ X_m^6 \\ X_m^7 \end{bmatrix} \tag{7}$$

which means that after removing the prefix-samples and performing a DFT in the receiver, the obtained samples are equal to the transmitted (`frequency-domain') symbols, up to a channel attenuation H_i (for tone-i). Hence channel equalization may be performed in the frequency domain, by component-wise divisions (divide by H_i for tone-i) (1-taps FDE).

The multi-path fading channel can be written as:

$$r = H_c x + v \tag{8}$$

The channel equalization issue will be investigated in OFDM. Let h(t) designate the channel impulse response and H(w) its Fourier transform, i.e., the channel transfer function. If the number of carriers is sufficiently large, the channel transfer function becomes virtually

nonselective within the bandwidth of each individual carrier. Focusing on one particular carrier, the influence of multipath fading reduces to attenuation and a phase rotation.

Referring back to the channel transfer function H(w), we let

$$\mathrm{H}_k = \rho_k . e^{j\theta_k} \tag{9}$$

Designate its value within the bandwidth of the *kth* carrier. Equalization of the channel requires that at the DFT output in the receiver, the *kth* carrier signal be multiplied by a complex coefficient

$$C_k = 1 / H_k \tag{10}$$

This is the result of an optimization based on the zero-forcing (ZF) criterion [14], which aims at canceling ISI regardless of the noise level. To minimize the combined effect of ISI and additive noise, the equalizer coefficients can be optimized under the minimum mean-square error (MMSE) criterion. This optimization yield

$$\mathrm{C}_k = \frac{\mathrm{H}_k^{*}}{\left|\mathrm{H}_k\right|^2 + \sigma_n^{\,2} / \sigma_a^{\,2}} \tag{11}$$

Where σ_n^2: is the variance of additive noise, and σ_a^2 is the variance of the transmitted data symbols. Note that the MMSE solution reduces to the ZF solution for of $\sigma_n^2 = 0$.

Channel equalization in OFDM systems thus takes the form of a complex multiplier bank at the DFT output in the receiver.

The ZF criterion does not have a solution if the channel transfer function has spectral nulls in the signal bandwidth. Inversion of the channel transfer function requires an infinite gain and leads to infinite noise enhancement at those frequencies corresponding to spectral nulls. In general, the MMSE solution is more efficient, as it makes a trade-off between residual ISI (in the form of gain and phase mismatchs) and noise enhancement. This is particularly attractive for channels with spectral nulls or deep amplitude depressions.

3.2. Frequency-domain equalization

Analyzing the operation principle of OFDM, Frequency domain equalization is illustrated in Figure 4a which shows the baseband equivalent model of a single-carrier system employing this equalization technique. The received signal samples are passed to an N-point DFT, each output sample is multiplied by a complex coefficient C_i, and the output is passed to an IDFT to transform the signal back to the time domain. Now, if we take the system sketched in Figure 4a and place it between an IDFT operator and a DFT operator, we obtain an OFDM system

incorporating a frequency domain equalizer. Obviously, the DFT and IDFT operators at the output end cancel each other, and the system simplifies to what we see in Figure 4b. This is precisely the schematic diagram of the equalized OFDM system discussed in the previous. Figures 4a and 4b give evidence of the strong similarities of OFDM signaling and frequency domain equalization in single-carrier systems. In cases, time/ frequency and frequency/ time transformations are made. The difference is that in OFDM systems, both channel equalization and receiver decisions are performed in the frequency domain, whereas in single-carrier systems the receiver decisions are made in the time domain although channel equalization is performed in the frequency domain.

In this section we study the performance MMSE equalizer rather than ZF over SUI MultiPath Channels, because the MMSE solution is more efficient [15]-[17], as it makes a trade-off between residual ISI (in the form of gain and phase mismatchs) and noise enhancement.

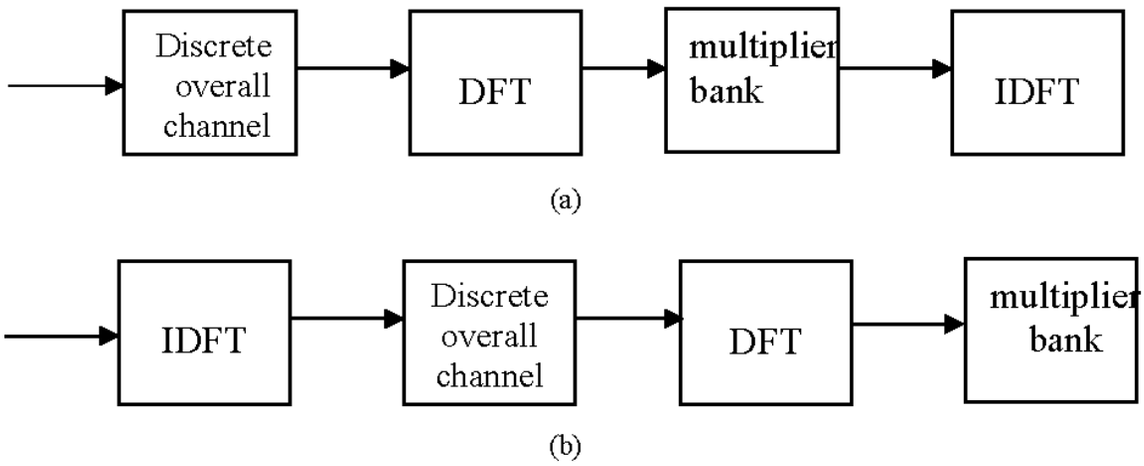

Figure 4. Frequency domain channel equalization. (a) Single carrier (b) OFDM

3.3. Simulation results

To compare the performance of OFDM systems in frequency selective fading channel, we consider OFDM block transmission over SUI channel model which is multipahs channel adopted by IEEE 802.16a task group for evaluating Broadband wireless system in 2-11 GHz bands. The sampling rate was assumed 20 Ms/sec.

This simulated system employs an OFDM signal with N =256, and 512 sub carriers using QPSK, 16 QAM, and 64 QAM, respectively.

In this simulation, SUI 1 from train type C(Flat/Light tree density), SUI3 from train type B(Hilly/ Light tree density or Flat/moderate tree density), and SUI 5 from train type A(Hilly/moderate to heavy tree density) are assumed for simplicity.

BER performance of OFDM system using MMES equalizer will be investigated in Figures 5, 6, 7, 8, 9,and 10 over SUI 1,3,5 channel models and AWGN for N=256 and 512 at 16QAM, 64 QAM and QPSK, respectively. Moreover, the performance of OFDM over SUI channel will be

http://dx.doi.org/10.5772/55380

compared with the AWGN only as shown in Figures 11 and 12 for N=256 and N=512, respectively.

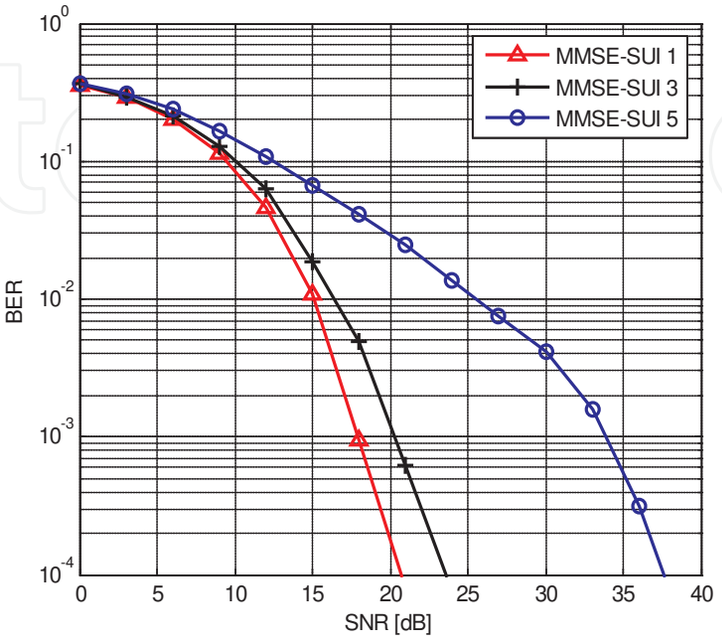

Figure 5. OFDM BER Performance (N=256, 16QAM)

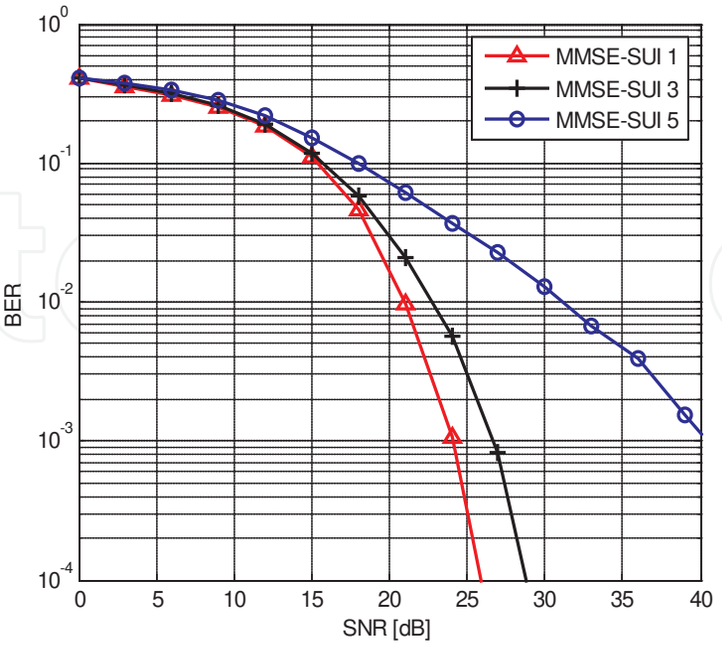

Figure 6. OFDM BER Performance (N=256, 64QAM)

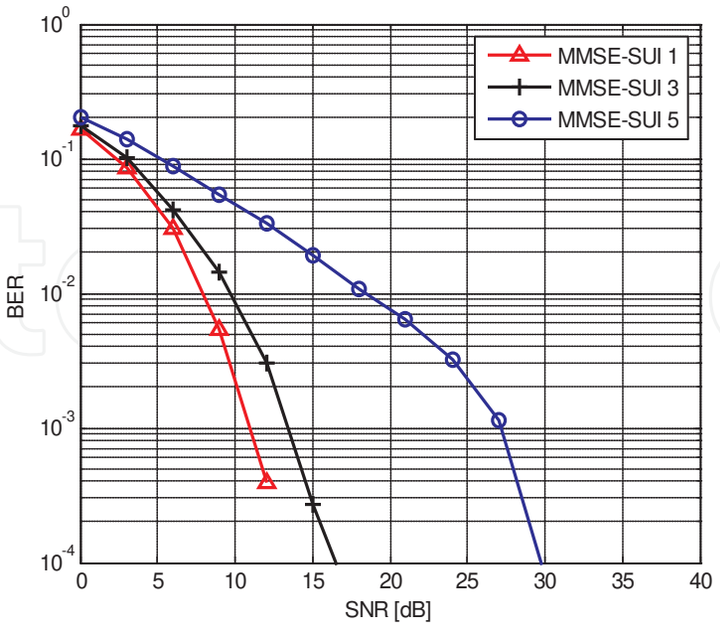

Figure 7. OFDM BER Performance (*N*=256, QPSK)

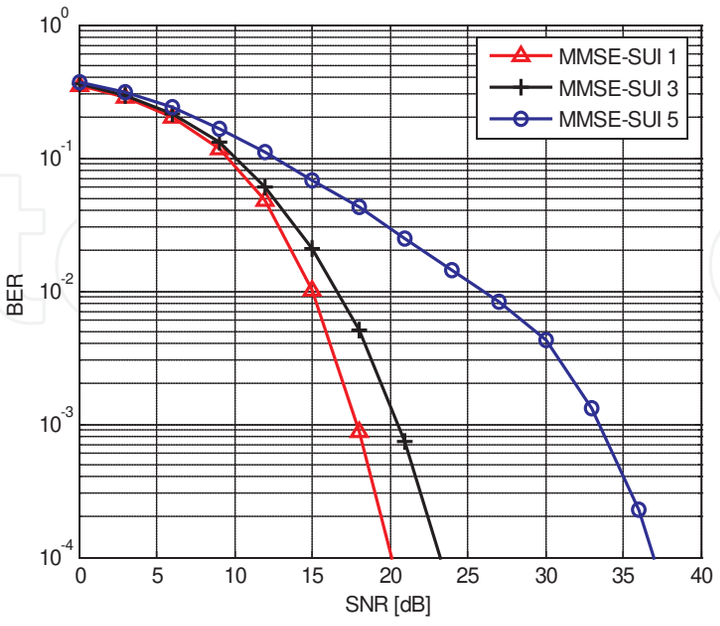

Figure 8. OFDM BER Performance (*N*=512, 16QAM)

http://dx.doi.org/10.5772/55380

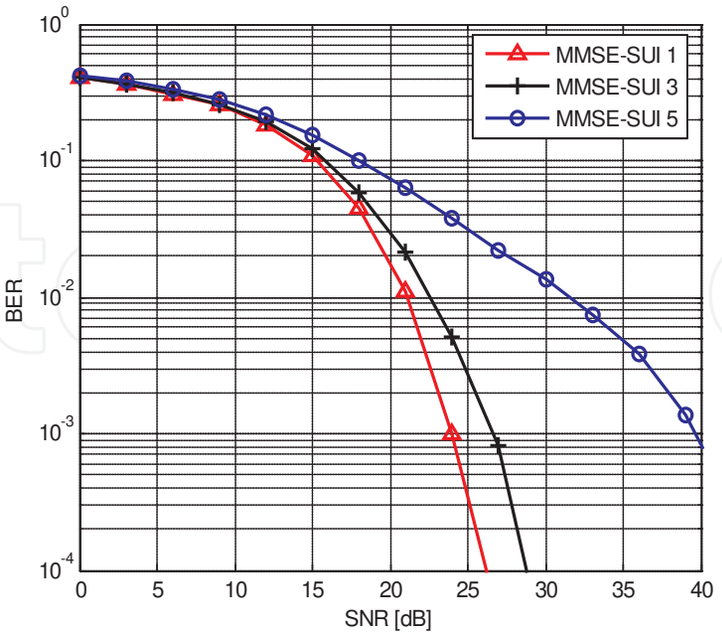

Figure 9. OFDM BER Performance (*N*=512, 64QAM)

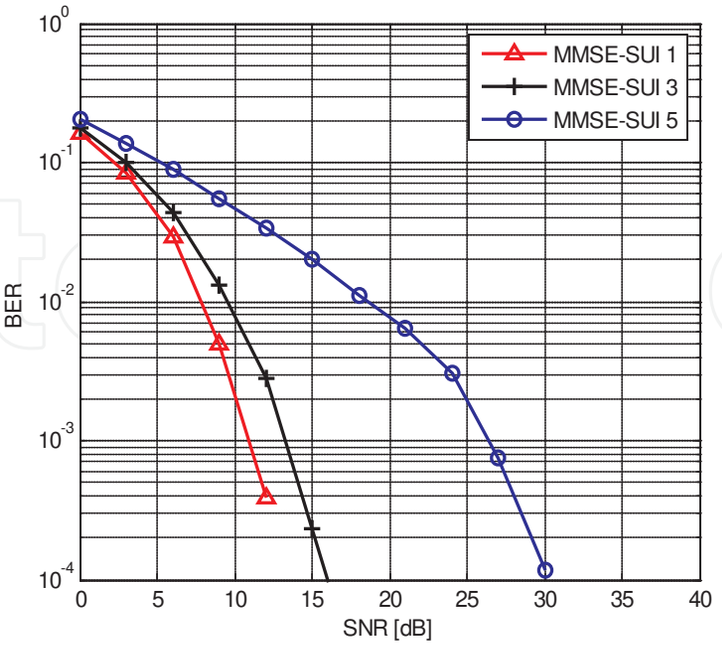

Figure 10. OFDM BER Performance (*N*=512, QPSK)

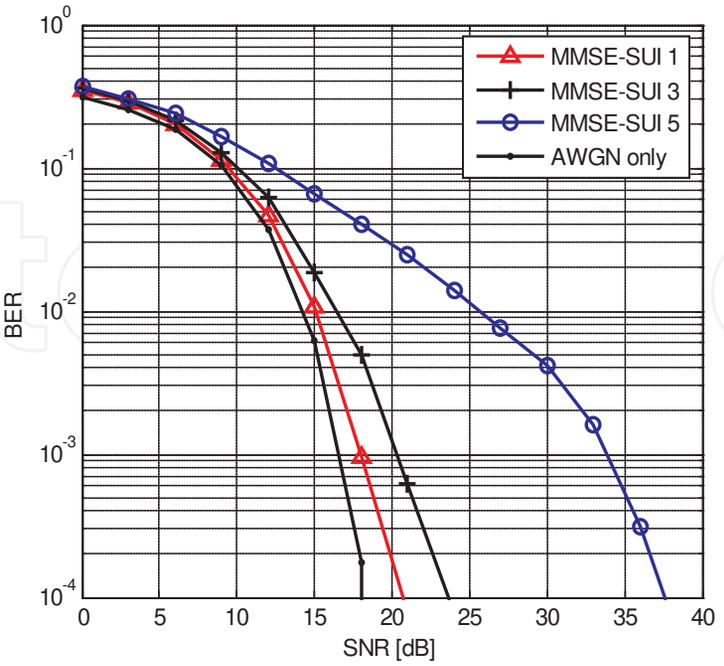

Figure 11. BER Performance comparison (16QAM, *N*=256).

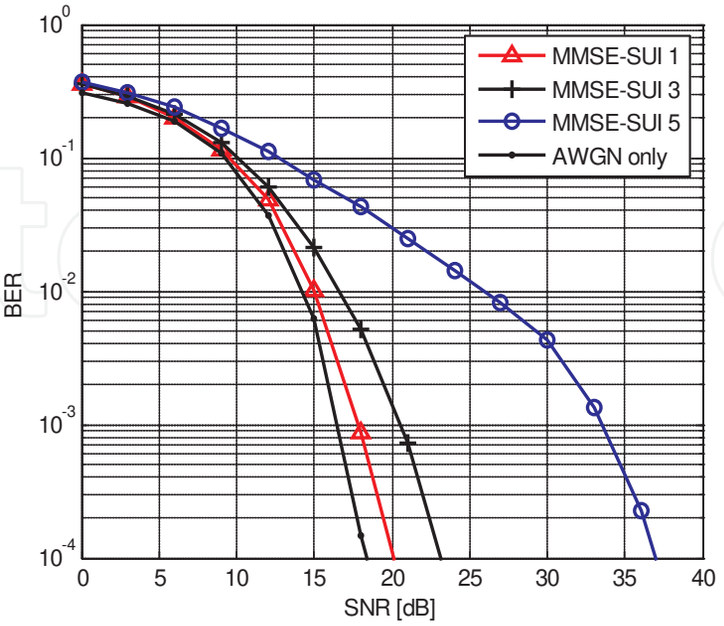

Figure 12. BER Performance comparison (16QAM, *N*=512).

http://dx.doi.org/10.5772/55380

4. WiMAX with compander for PAPR reduction

The system will be used in this work is shown in Figure 13. The transmitter section maps a random data bit sequence, into a sequence of QAM symbols. The QAM symbols are partitioned into N-length blocks and modulated onto the sub-carriers of an OFDM modulator via the inverse Fast Fourier Transform (IFFT). Before guard interval insertion, prior to transmission, the signal is companded with μ-law compander. The companded signal is then passed through the amplifier at the transmitter, which distorts the signal according to nonlinear solid state power amplifier models. After transmission, the signal is passed through SUI channels and corrupted with AWGN, compensation, μ-law expansion, and OFDM demodulation.

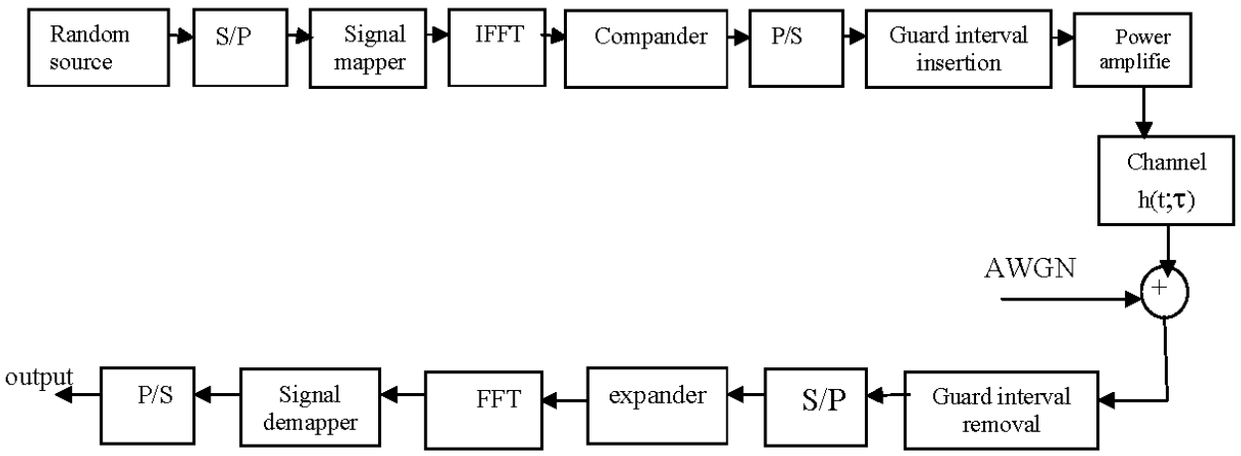

Figure 13. Simulation model of WiMAX system.

Compander (μ) was described in detail in chapter 3 where μ is the parameter controls the amount of compression.

5. Simulation results

The performance of proposed WiMAX is evaluated using computer simulation. In this study, the channel is assumed to be known perfectly at the receiver. The simulated system employs an OFDM signal with $N = 256$ subcarriers, among which *192* data carriers (*QPSK, 16QAM or 64QAM* signal mapping), *8* pilots, the others are nulls, guard interval $T_g = (1/4)T_b$, where T_b is the useful symbol time, and sampling frequency=9.12 *MHz*. For simplicity, uncoded OFDM will be employed. When applying the compander/expander, we must take into account some system constraints: Neither the pilots nor the guard intervals are allowed to be modified, for reasons of standard compliance.

5.1. CCDF performance

Figure 14 shows the performance improvement of the proposed system over a conventional system, i.e., without PAPR reduction, for the μ- law for different value of μ using 16 QAM signal mapping. At the probability of 10^{-3}, the PAPR is almost 1.1 dB, 2.55 dB, 4 dB and 4.5 dB smaller than conventional system, for μ=2, μ=4, μ=13 and μ=64, respectively. The same results are obtained when A-law is considered. Figure 15 shows the CCDF performance of the companding method at μ=13 compared with that of the system that is used clipping technique for reduction where CR = 2.

Figures 16 and 17 show the improvements which are obtained when 64 QAM and QPSK modulation are used, respectively.

5.2. BER performance

The BER performance of proposed WiMAX is evaluated here. In this study, the channel is assumed to be known perfectly at the receiver. The modulated signal is affected by SUI multipath channels and AWGN. Figure 18 shows the effect of different values of μ on the proposed system. In the following μ=13 is chosen to compromise between CCDF and BER performance. In Figure 19, at BER=10^{-4}, SNR over SUI 1 decreases by 8.2 dB better than the conventional system. The amount of improvement in SNR at BER=10^{-4} over SUI 3 and SUI 5 is 7.8 dB,and 5.2 dB better than the conventional system by using μ- law as shown in Figures 20 and 21, respectively.

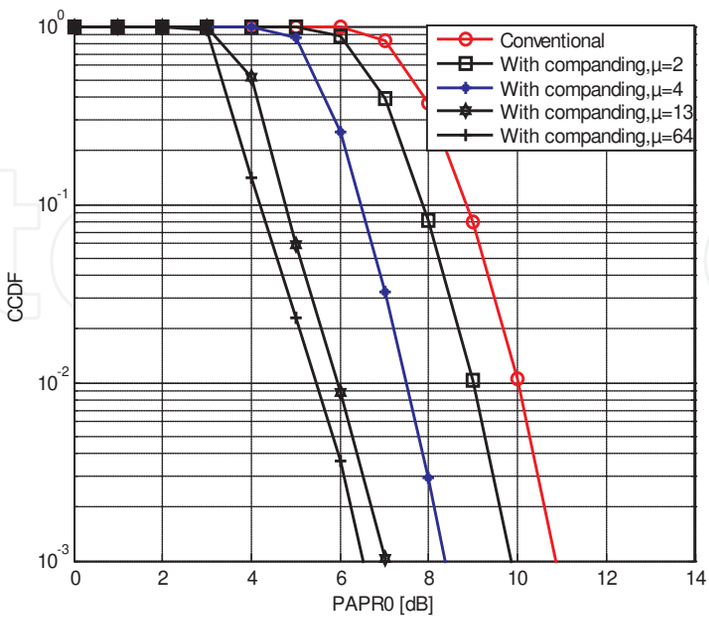

Figure 14. CCDF of PAPR with different μ (16-QAM constellation)

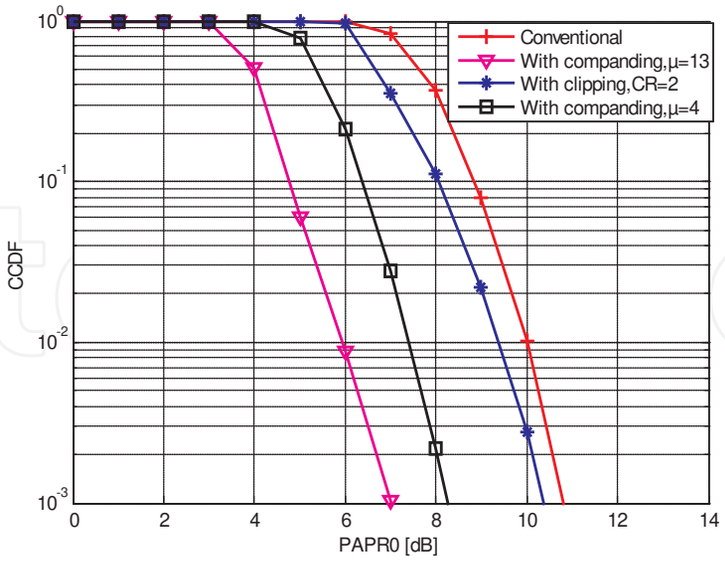

Figure 15. CCDF Performance comparisons with 16QAM.

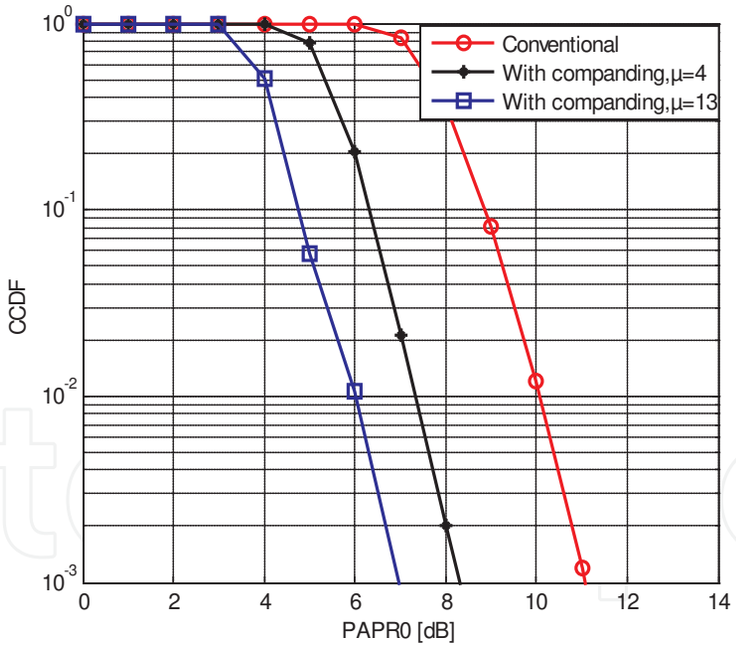

Figure 16. CCDF of PAPR with the proposed system (64QAM).

Figure 22 shows the system performance over AWGN only, where the amount of improvement in SNR is 10.7 dB at BER=10^{-4} than the conventional system. The BER performance of the companding method compared with the system that is used clipping technique where CR = 2 and CR=1.4 is shown in Figure 23.

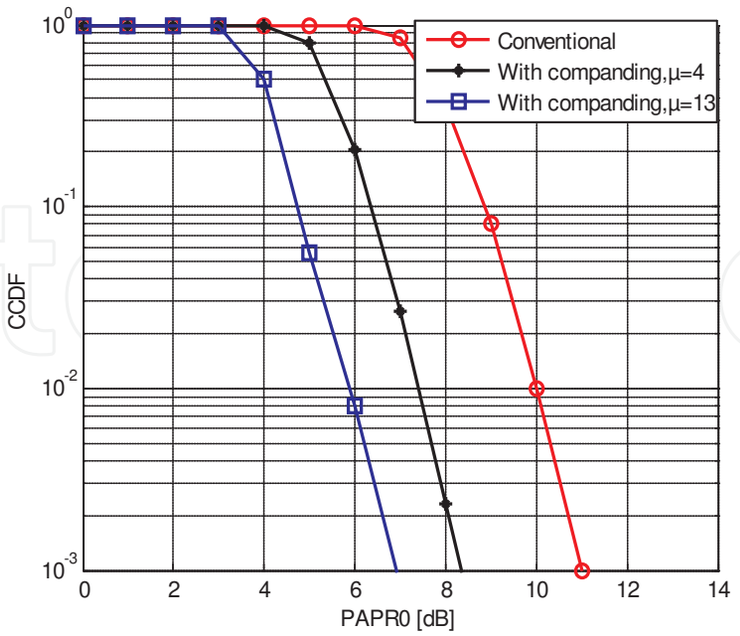

Figure 17. CCDF of PAPR with the proposed system (QPSK).

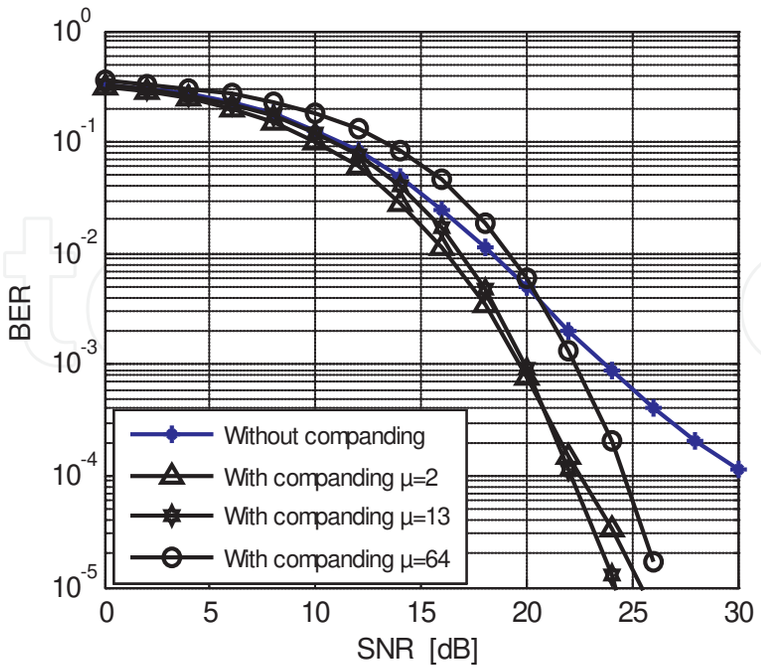

Figure 18. BER Performance with different μ.

http://dx.doi.org/10.5772/55380

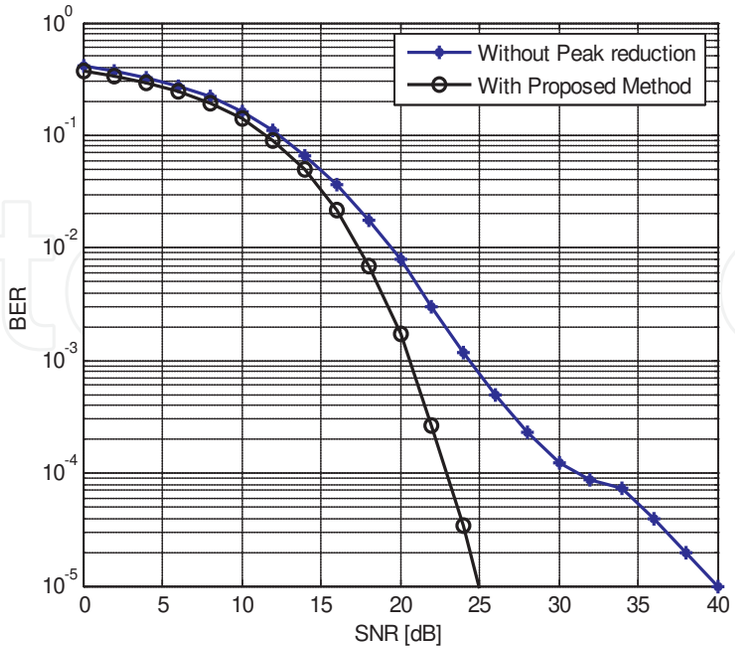

Figure 19. BER Performances over SUI 1 and AWGN.

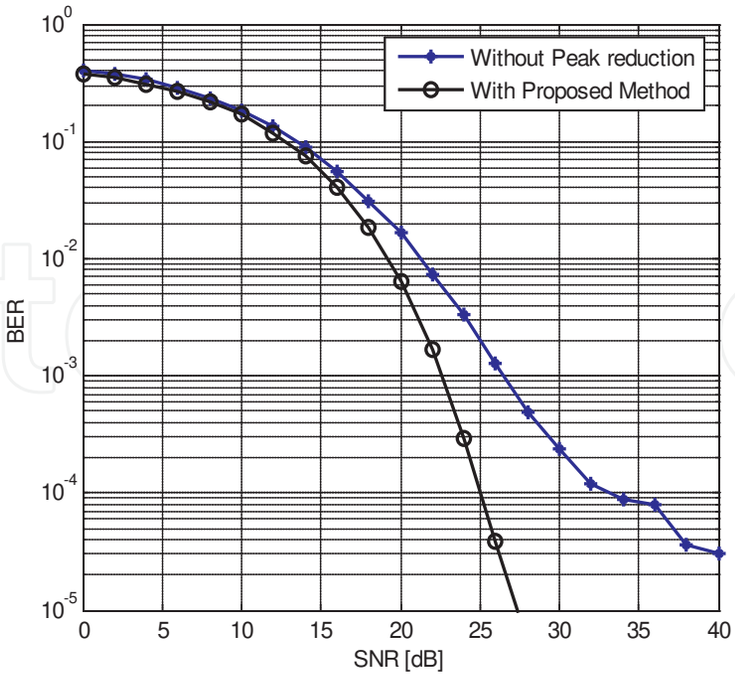

Figure 20. BER Performance over SUI 3 and AWGN.

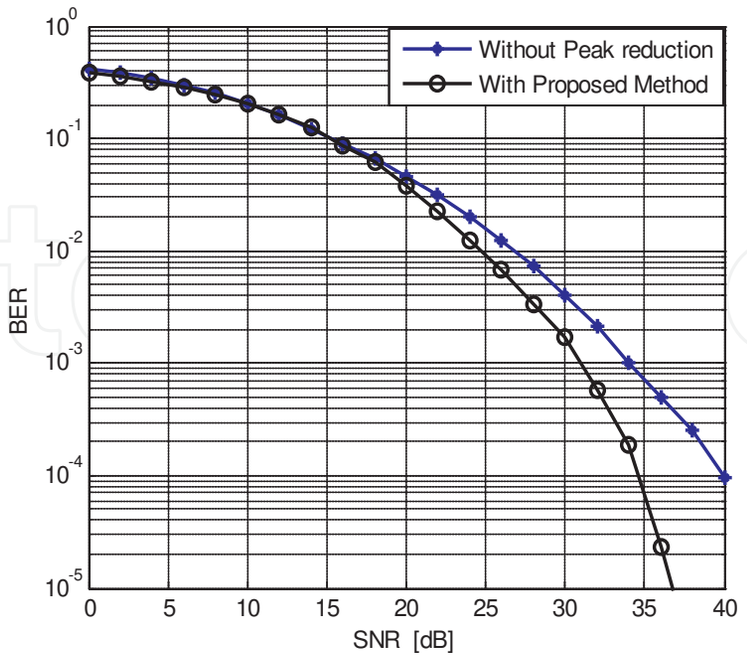

Figure 21. BER Performances over SUI 5 and AWGN.

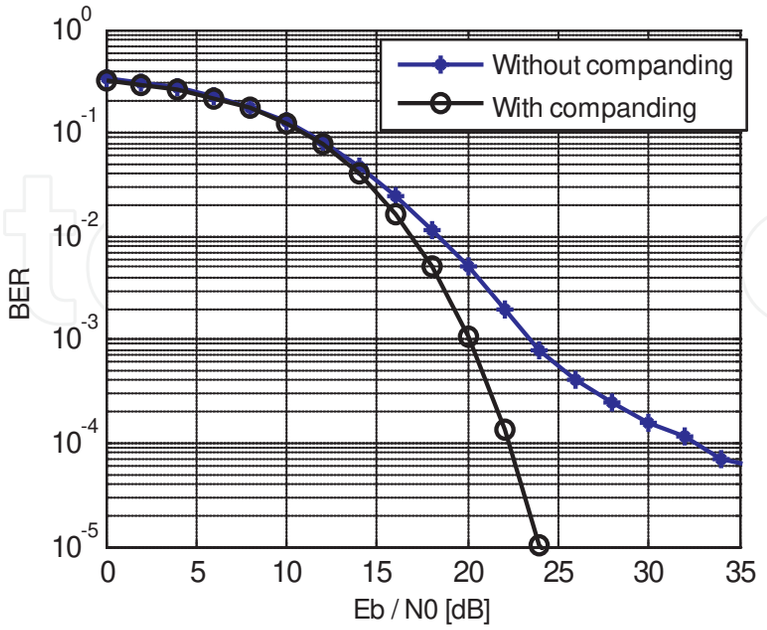

Figure 22. BER Performance over AWGN only.

http://dx.doi.org/10.5772/55380

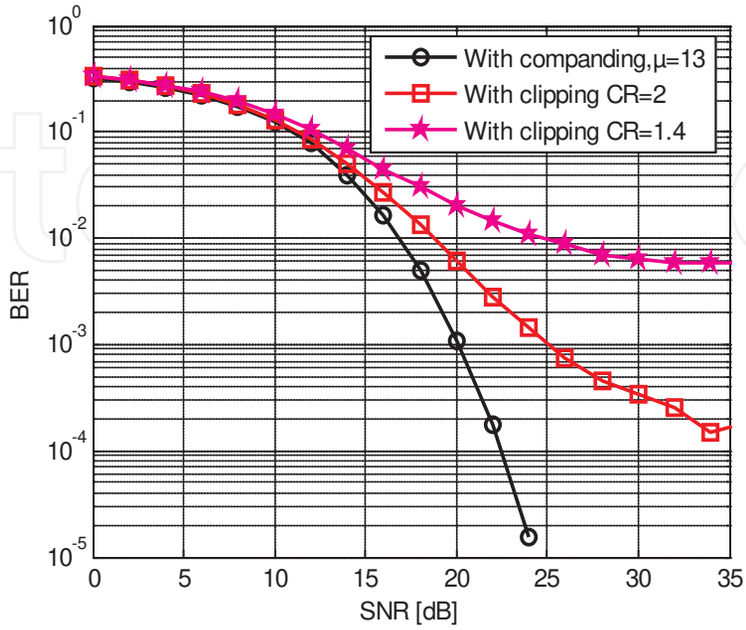

Figure 23. BER Performance comparisons.

6. Summary

We have investigated the PAPR in the WiMAX system. We investigates the simulation performance of WiMAX OFDM PHY Layer in the Presence of Nonlinear Power Amplifier and the new method is suggested to reduce PAPR where the simulation results show that, the peak power reduces by about 4 dB and SNR also decreases more than 5 dB at BER =$10^{-4.}$ The Stanford University Interim (SUI) channel models are selected for the wireless channel in the simulation. Moreover the equalizer performance with SUI multipaths channel is explained.

Author details

Mona Shokair* and Hifzalla Sakran

*Address all correspondence to: shokair_1999@hotmail.com i_shokair@yahoo.com

Dept. of Electrical Communication, Faculty of Electronic Engineering, El-Menoufia University El-Menoufia, Egypt

References

[1] IEEE 802.16 and WiMAX. http://www.wimax industry.com/wp/papers/intel_80216_wimax.pdf (accessed 15 Decmber 2008).

[2] A Ghosh, D R Wolter, J G Andrews, and R Chen. Broadband Wireless Access with WiMax/802.16: Current Performance Benchmarks and Future Potential. IEEE Communications Magazine Feb. 2005; 43(2) 129-136.

[3] I Koffman, and V Roman. Broadband Wireless Access Solutions Based on OFDM Access in IEEE 802.16. IEEE Communications Magazine April. 2002; 40(4) 96-103.

[4] ETSI Broadband Radio Access Networks (BRAN); HIPERMAN; Physical (PHY) Layer. Standard TS 102 177, 2003.

[5] F H Gregorio. Analysis and Compensation of Nonlinear Power Amplifier Effects in Multi Antenna OFDM Systems. PhD thesis, Helsinki University of Technology, Finland; Nov. 2007.

[6] K Gorazd, J Tomaz, J Igor, and P Sreco. Effects of Nonlinear High Power Amplifier on the Area Covered by WiMAX Signal. IEEE Sarnoff Symposium : Conference Proceedings: March 2006.

[7] H Xiong, P Wang, and Z. Bu. An Efficient Peak-to-Average Power Ratio Reduction Algorithm for WiMAX System. Asia-Pacific Conference on Communications :Conference Proceedings: Aug. 2006.

[8] C Wei, Y Tianren, and W Hui. A New Method for Reduction of PAPR Using CORDIC Algorithm in WiMAX System. International Conference on Communications, Circuits and Systems : Conference Proceedings: 2006.

[9] S Hu, G Wu, J Ping, and S Li. HPA Nonlinearity Reduction by Joint Predistorter and Tone-Reservation with Null Subcarriers in WiMAX Systems. 4th IEEE International Conference on Circuits and Systems for Communications : Conference Proceedings: May 2008.

[10] S Haykin. Communication Systems. 4Th Edition John Wiley&Sons: In Tech; 2011.

[11] V Erceg. An Empirically Based Path Loss Model for Wireless Channels in Suburban Environments. IEEE JSAC July 1999; 17(7) 1205-1211.

[12] V Erceg, K V S Hari, M S Smith, and D S Baum. Channel Models for Fixed Wireless Applications. IEEE 802.16.3 Feb. 2001; Task Group Contributions.

[13] A Goldsmith. Wireless Communications. Cambridge University Press: In Tech; 2005.

[14] D Falconer, S L Ariyavisitakul, A B Seeyar, and B Edison. Frequency Domain Equalization for Single-Carrier Broadband Wireless Systems. IEEE Magazine of Communication April 2002; 40(4) 58-66.

[15] W Jeon, K Chang, and Y Cho. An Equalization Method for Orthogonal Frequency Division Multiplexing system in Time-Variant Multipath Channels. IEEE transactions on communications January 1999; 47(1).

[16] J Rinne, and M Renfors. An Equalization Method for Orthogonal Frequency Division Multiplexing System in Channels with Multipath Propagation Frequency Offset and Phase Noise. IEEE Global Telecommunications Conference : Conference Proceedings: 1996; 96(2) 1442–1446.

[17] H Sari, G Karam, and I Jeanclaudle. Frequency-Domain Equalization of Mobile Radio and Terrestrial Broadcast Channels. IEEE Global Telecommunications Conference : Conference Proceedings: 1994; 94(1) 1 – 5.

IntechOpen